ORIGINAL RESEARCH

Synthesis, characterization, and antimicrobial properties of novel double layer nanocomposite electrospun fibers for wound dressing applications

Alaa J Hassiba[1]
Mohamed E El Zowalaty[2]
Thomas J Webster[3–5]
Aboubakr M Abdullah[6]
Gheyath K Nasrallah[7]
Khalil Abdelrazek Khalil[8]
Adriaan S Luyt[6]
Ahmed A Elzatahry[1]

[1]Materials Science and Technology Program, College of Arts and Sciences, Qatar University, Doha, Qatar; [2]School of Health Sciences, University of KwaZulu-Natal, Durban, South Africa; [3]Department of Chemical Engineering, [4]Department of Bioengineering, Northeastern University, Boston, MA, USA; [5]Center of Excellence for Advanced Materials Research, King Abdulaziz University, Jeddah, Saudi Arabia; [6]Center for Advanced Materials, [7]Department of Biomedical Science, College of Health Sciences, Biomedical Research Center, Qatar University, Doha, Qatar; [8]Department of Mechanical Engineering, College of Engineering, University of Sharjah, Sharjah, United Arab Emirates

Correspondence: Ahmed A Elzatahry
Materials Science and Technology Program, College of Arts and Sciences, Qatar University, Doha 2713, Qatar
Email aelzatahry@qu.edu.qa

Abstract: Herein, novel hybrid nanomaterials were developed for wound dressing applications with antimicrobial properties. Electrospinning was used to fabricate a double layer nanocomposite nanofibrous mat consisting of an upper layer of poly(vinyl alcohol) and chitosan loaded with silver nanoparticles (AgNPs) and a lower layer of polyethylene oxide (PEO) or polyvinylpyrrolidone (PVP) nanofibers loaded with chlorhexidine (as an antiseptic). The top layer containing AgNPs, whose purpose was to protect the wound site against environmental germ invasion, was prepared by reducing silver nitrate to its nanoparticulate form through interaction with chitosan. The lower layer, which would be in direct contact with the injured site, contained the antibiotic drug needed to avoid wound infections which would otherwise interfere with the healing process. Initially, the upper layer was electrospun, followed sequentially by electrospinning the second layer, creating a bilayer nanofibrous mat. The morphology of the nanofibrous mats was studied by scanning electron microscopy and transmission electron microscopy, showing successful nanofiber production. X-ray diffraction confirmed the reduction of silver nitrate to AgNPs. Fourier transform infrared spectroscopy showed a successful incorporation of the material used in the produced nanofibrous mats. Thermal studies carried out by thermogravimetric analysis indicated that the PVP–drug-loaded layer had the highest thermal stability in comparison to other fabricated nanofibrous mats. Antimicrobial activities of the as-synthesized nanofibrous mats against *Staphylococcus aureus*, *Escherichia coli*, *Pseudomonas aeruginosa*, and *Candida albicans* were determined using disk diffusion method. The results indicated that the PEO–drug-loaded mat had the highest antibacterial activity, warranting further attention for numerous wound-healing applications.

Keywords: nanomaterials, wound dressing, nanofibers, electrospinning, biomedical, antimicrobial, activity

Introduction

Electrospinning is a simple and cost-effective technique used to fabricate fibers with a diameter on the nanometer scale.[1] Electrospun nanofibers have been studied extensively for their potential benefits in tissue scaffolding,[2,3] drug release,[4–6] and wound dressings.[7–9] Wound dressings with nanofibrous materials contribute to improved hemostasis, absorption of exudates from the wound, flexibility in the designed dressing mat, and maintenance of moisture in the wound environment, allowing for oxygen and water permeability.[10] Their greatest potential, however, lies in their physical features as electrospun nanofibers have large surface area to volume ratios, high porosity containing small pores, and a matrix morphology that resembles the natural extracellular matrix of the human body.[11,12]

The use of composite nanofibrous mats in wound dressing applications is of more interest in comparison to the pristine mats because of their enhanced properties. According to the literature, the majority of electrospun composite nanofibrous mats have been fabricated using blends[13,14] or in the form of core-shells.[15] Nevertheless, relatively less research has been conducted on sequential electrospinning to create a multilayered wound dressing electrospun nanofibrous mat.[16]

Sirc et al prepared a multilayered structure of the nanofibers using Nanospider™ needleless technology. The mat consisted of two polyurethane layers sandwiching a poly(vinyl alcohol) (PVA) layer, which held the antibiotic gentamicin. Mats with differing polyurethane thickness values were fabricated, demonstrating that an increase in layer thickness contributed to the prolonged release of gentamicin.[17] Chen et al created a nanofibrous multilayered structure of poly(D,L-lactide-co-glycolide and collagen that contained vancomycin, gentamicin, and lidocaine to repair infected wounds. The study included conditions in which the electrospun mats were prepared, an in vitro test and an in vivo investigation completed on rat wounds.[18] This multilayered mat proved to be effective at facilitating wound healing at an early stage. More recently, Tan et al developed a bilayered wound dressing consisting of polyurethane and gelatin; the double layer used in their investigation showed desirable performance in terms of water vapor transmission rate and water absorption ratio with hemostatic and antibacterial properties.[16]

A commonly studied polymer in fabricating wound dressing mats is chitosan. Chitosan is a natural polymer that is biodegradable and biocompatible at a low cost. Furthermore, it has polycationic properties that allow it to act as an antimicrobial with a wide spectrum of antibacterial activity. Chitosan has also been proven to enhance tissue regeneration and hemostasis.[19–21] However, pure chitosan is not an easily obtained electrospun nanofiber due to its high viscosity in the solution. Hence, to obtain nanofibers, chitosan can be mixed with readily spun polymers such as PVA[7,22,23] and polyethylene oxide (PEO).[24] PVA is considered as one of the oldest and most frequently used synthetic polymers with good biocompatibility properties.[25]

In order to enhance the antibacterial activity of dressing mats against both drug-sensitive and drug-resistant pathogenic bacteria, Lee et al incorporated silver nanoparticles (AgNPs) into a blend of chitosan and PVA polymeric mats.[26] The fibers showed a strong antibacterial inhibitory effect on *Escherichia coli* and *Staphylococcus aureus*

because of the AgNPs. The results also showed that PVA/chitosan/AgNPs should be more effective than PVA/chitosan/silver nitrate as wound dressing mats due to the leading performance of the AgNPs in the in vitro and in vitro animal experiments.

In general, wounds are repaired by the natural healing process; however, wound infections can be particularly problematic to this process. Consequently, the addition of drugs to the composite nanofibrous mat is essential to provide a septic environment for the injured site to heal more easily. There are several therapeutic agents or antibiotics that have been used to serve this purpose, such as gentamicin sulfate,[27] minocycline,[28] norfloxacin,[29] and chlorhexidine.[30,31] Chlorhexidine is an antiseptic included in several biomedical applications, including disinfectants and antibacterial agents that are non-toxic to mammalian cells, due to its subsensitivity for skin, low irritation, and role against a wide range of microorganisms such as Gram-negative and Gram-positive bacteria and fungi.[32,33]

In this article, we propose a novel double-layer electrospun nanocomposite nanofibrous mat for wound dressing applications serving a dual function. The first layer of the mat, which is exposed to the environment, consists of PVA/chitosan/AgNPs. Although this layer has been reported as an effective antibacterial nanofibrous mat for wound dressing,[26] there are possible negative effects from exposure to AgNPs, due to their unique distribution patterns in vivo. Furthermore, surface chemistry is also of concern as it is still poorly understood at this point.[34,35] In this investigation, AgNPs were used as an upper layer, which played a protective role against environmental germs blocking microbial invasion to the injured site. The second layer, which is in direct contact with the injured site, is composed of electrospun PEO or polyvinylpyrrolidone (PVP) nanofibers incorporated with chlorhexidine as a model antimicrobial (antiseptic) compound. The involvement of chlorhexidine in this layer inhibits the bacterial growth at the wound site that would otherwise obstacle the healing process.

Materials and methods
Chemicals
PVA (molecular weight 89,000–98,000, 99+% hydrolyzed) was obtained from Sigma-Aldrich. Chitosan (medium molecular weight) was purchased from Sigma-Aldrich. The $AgNO_3$ was obtained from Sigma-Aldrich. PVP (molecular weight 1,300,000) was obtained from Sigma-Aldrich. PEO (molecular weight 200,000) was acquired from Sigma-Aldrich. Aqueous acetic acid (≥99.7%) was also obtained from Sigma-Aldrich. All reagents were used without further

purification. Double-distilled water was used to prepare all polymer solutions.

Preparation of electrospinning solutions

First layer
Initially, a PVA solution with a concentration of 8 wt/wt% was prepared by dissolving the polymer in distilled water (80°C) using magnetic stirring until the solution was clear. Chitosan solution was prepared by dissolving the polymer in 2 v/v% acetic acid using magnetic stirring at a temperature of 60°C until the solution was clear. PVA/chitosan with a concentration of 12/4.7 wt/wt% was prepared by adding chitosan to PVA, while continuing to stir using magnetic stirring to ensure the production of homogeneous solutions. Subsequently, silver nitrate was added to the dissolved polymers to create a PVA/chitosan/AgNO$_3$ solution. It should be noted that an added 0.0198 g of silver nitrate yields 0.0126 g of silver.

Second layer
PVP (12 wt%) was prepared by dissolving the polymer in distilled water at room temperature. Chlorhexidine (5 wt%) was added to the solution and kept on stirring at room temperature until a clear solution was formed.

PEO (8 wt%) was prepared by dissolving the polymer in chloroform at room temperature. Chlorhexidine (5 wt%) was added to the solution and stirred continuously at room temperature until a clear solution was formed.

Electrospinning
The prepared solutions were placed in a syringe of size 5 mL. A tube was connected from the syringe, from one end, to the needle (gauge 23). Underneath the needle, a piece of aluminum foil was placed where the sample will be collected. Both the tip of the needle and the collector were connected to a high power supply. The electrospun fibers were obtained at an applied voltage of 18 kV and at 10 cm collection distance. The first layer, which contained PVA/chitosan/AgNPs, was followed by the deposition of drug-loaded PVP or PEO in the second layer.

Characterization
The morphology and diameter of the electrospun nanofiber mats were observed via an FEI Quanta 200 scanning electron microscopy (SEM) (FEI, Hillsboro, OR, USA). Small sections of the sample were cut, and Agar sputter coater was utilized to sputter a layer of gold over the sample. The morphology of the nanoparticles was studied using transmission electron microscope (TEM) images. Images were obtained using an FEI Tecnai GF S-Twin TEM (FEI). Samples were prepared by sonicating the nanofiber mat in ethanol for 2 hours. The solvent was dropped and dispersed on a carbon-coated grid. Following solvent evaporation, samples were processed for TEM. Fourier transform infrared spectroscopy (FT-IR) characterization was performed using a Spectrum 400 FT-IR/FT-NIR Spectrometer (PerkinElmer). The wavelength range was set from 4,000 to 400 cm^{-1} to allow for analysis of the functional groups of the electrospun nanofibers. Thermogravimetric analysis (TGA) measurements were performed using a thermogravimetric analyzer – Pyris 6 (PerkinElmer). For each measurement, 2–7 mg of electrospun polymer was loaded into a platinum pan, and weight loss was recorded at a rate of 10°C/min starting at room temperature up to 600°C in a dry nitrogen environment. An X-ray diffraction (XRD) technique was used to study the crystallinity of the sample and was carried out using a MiniFlex Desktop X-ray Diffractometer (Rigaku Corporation, Tokyo, Japan). The parameters used were as follows: source current 15 mA, voltage 30 kV, wavelength 1.5404 Å, and the start and stop angles 5° and 80°, respectively.

Microorganisms and culture media
In this study, four microbial species were used: Gram-positive bacteria, *S. aureus* (ATCC BAA-976); Gram-negative bacteria, *E. coli* (ATCC 8739); *Pseudomonas aeruginosa* (ATCC BAA-1744); and *Candida albicans* (ATCC 10231). They were obtained from the American Type Culture Collection and were cultured on LB agar (Lennox L; Invitrogen).

Antimicrobial sensitivity test
Antimicrobial activity was investigated against the chosen microorganisms using the disk diffusion method as described previously.[36] The McFarland 3 turbidity standard was used as a reference to inoculate fresh LB Agar plates with 9×10^8 colony forming units (CFUs) of each microorganism in broth, which were later evenly spread on the medium surface. A 7 mm diameter disk was obtained from each membrane sample and placed onto the inoculated plates and incubated at 37°C for 18 hours.

Results and discussion

Characterization

SEM
The morphology of the external upper layer is depicted in Figure 1. Spindle-like beaded fiber with an average fiber diameter of 200.0–250.0 nm under the same conditions of 18 kV applied power and 10 cm collecting distance was
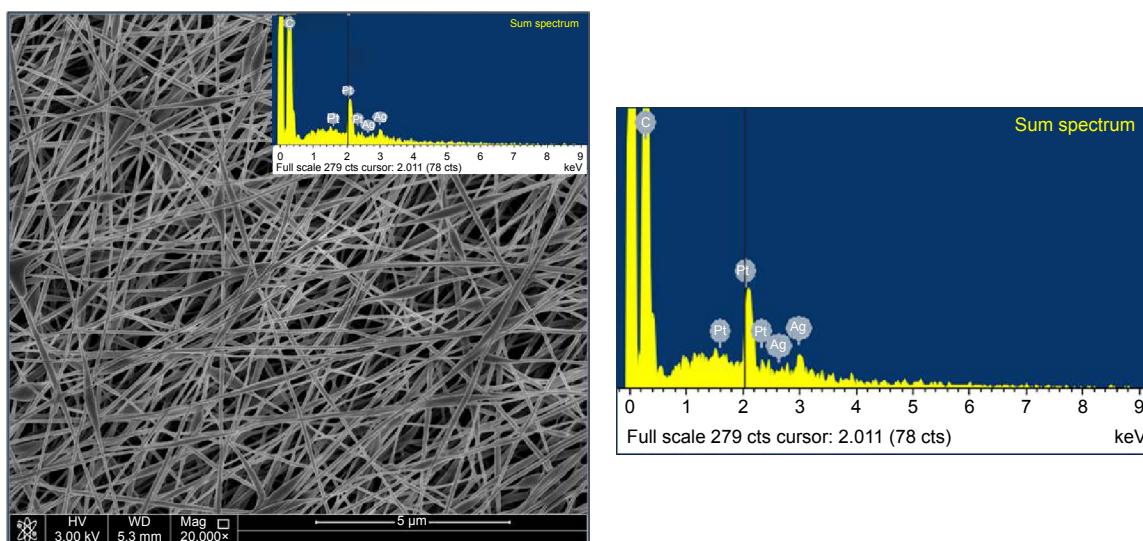
Figure 1 SEM image of fabricated electrospun mat.
Notes: SEM image at 20,000× of electrospun nanofibers of PVA/chitosan/AgNPs blends of 12 wt%/0.6 wt%/0.9 wt%, respectively, using the following electrospinning conditions of 10 cm, 18 kV, and 0.3 mL/h. The EDS was collected on the PVA/chitosan/AgNPs.
Abbreviations: SEM, scanning electron microscopy; PVA, poly(vinyl alcohol); AgNPs, silver nanoparticles; EDS, energy dispersive spectrum; wt, weight; HV, high voltage; Mag, magnification; WD, working distance.

observed. In addition, the identification of Ag as an elemental component was detected using the energy dispersive spectrum (EDS) as shown in Figure 1. Two peaks were relatively weak, but indicated the presence of Ag. The same conditions led to a uniform and homogeneous fiber in case of PVP (Figure 2) and nonhomogeneous fiber in case of PEO (Figure 3).

TEM
TEM was conducted on PVA/chitosan/AgNPs samples to investigate the presence of AgNPs. TEM images of the

sample are presented in Figure 4. Nanofibers were successfully obtained, and the size of silver grains captured showed that the loaded silver particles are in the nanosize.

FT-IR
FT-IR was used to characterize the presence of specific chemical groups in the materials. Each wavelength corresponded to the unique chemical bonds in the material. Furthermore, the size of the produced peaks was related to the amount of the material present.[37] Figure 5 shows the FT-IR results
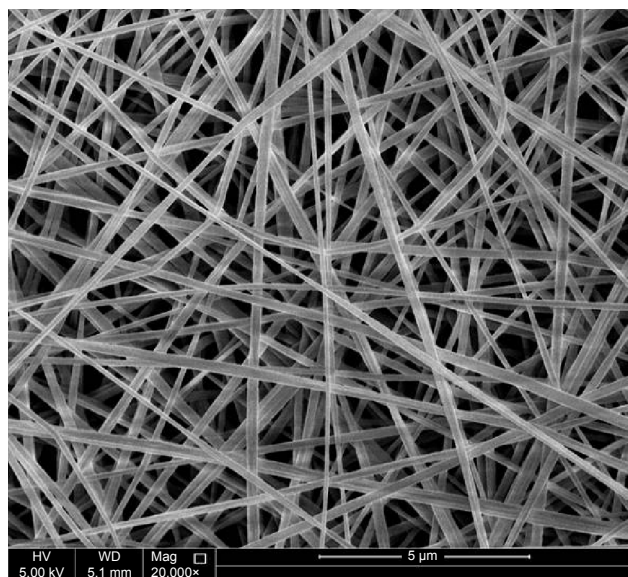

Figure 2 SEM image of fabricated electrospun mat.
Note: SEM image at 20,000× of electrospun nanofibers of PVP 12% (wt/v) using the following electrospinning conditions of 10 cm, 18 kV, and 0.3 mL/h.
Abbreviations: SEM, scanning electron microscopy; PVP, polyvinylpyrrolidone; v, volume; wt, weight; HV, high voltage; Mag, magnification; WD, working distance.
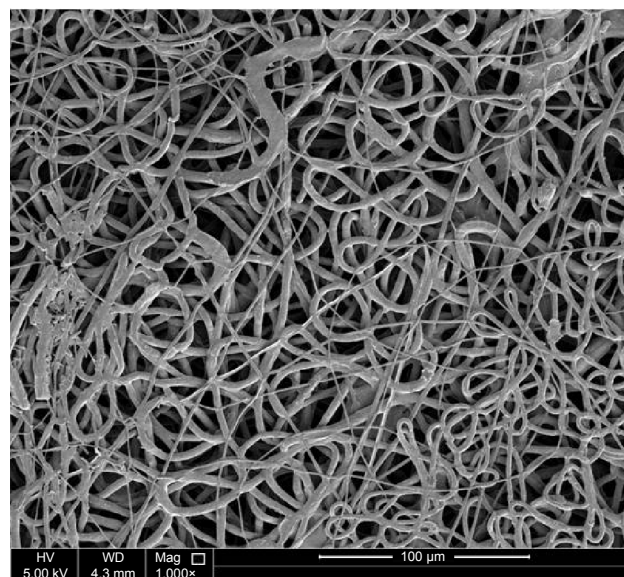

Figure 3 SEM image of fabricated electrospun mat.
Note: SEM image at 1,000× of electrospun nanofibers of PEO 8% (wt/v) using the following electrospinning conditions of 10 cm, 18 kV, and 0.3 mL/h.
Abbreviations: SEM, scanning electron microscopy; PEO, polyethylene oxide; v, volume; wt, weight; HV, high voltage; Mag, magnification; WD, working distance.
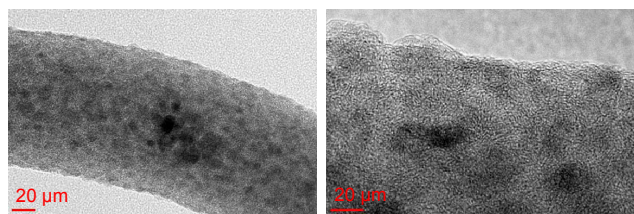
Figure 4 TEM image showing AgNPs on a nanofiber.
Abbreviations: TEM, transmission electron microscopy; AgNPs, silver nanoparticles.

for the following samples: pure PVA, pure chitosan, PVA/ chitosan, PVA/chitosan/AgNPs, PVP–drug-loaded double layer, and PEO–drug-loaded double layer.

The spectrum of PVA (Figure 5A) showed the typical absorption band occurring at 3,300 cm^{-1}, demonstrating OH stretching. The band at 2,940 cm^{-1} indicates the asymmetric and symmetric stretching of CH$_2$. At 1,140 cm^{-1}, stretching of CO from the crystalline sequence of PVA is shown.[38] The spectrum of chitosan (Figure 5B) shows characteristic absorption bands at ~2,872 and 3,319 cm^{-1}, which is ascribed for the –CH$_3$ and –OH groups, respectively. The band at 1,152 cm^{-1} is attributed to the glycosidic bonding.[39] The spectrum of PVA/chitosan (Figure 5C) shows the characteristic absorption bands for pure PVA in addition to the absorption bands, which are characteristic of the chitosan sample. The spectrum of PVA/chitosan/AgNPs (Figure 5D) indicates that the AgNPs were well stabilized in the mixture without deterioration of functional groups.

The spectrum of PVA/chitosan/AgNPs/PVP/chlorhexidine (Figure 5E) shows the characteristic absorption bands for pure PVA, pure chitosan, and the additional absorption bands
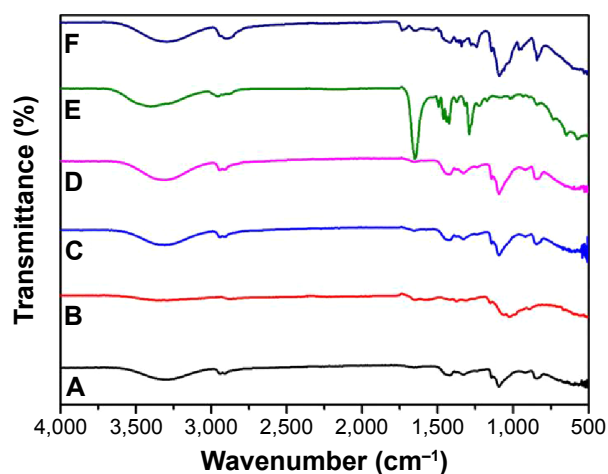
characteristic of PVP and of chlorhexidine. It can be observed that the intensity of the peak between 1,000 and 1,200 is lower compared to the peak in the spectra (A), (B), (C), and (D). The additional band characteristics of PVP appear at 1,647 cm^{-1}, which accounts for the carbonyl (C=O) stretching affected by hydrogen bond formation with water molecules.[40] The additional band characteristics of chlorhexidine appear at 1,492 cm^{-1}, which is related to the chlorophenol groups of chlorhexidine.[41]

The spectrum of PVA/chitosan/AgNPs/PEO/chlorhexidine (Figure 5F) shows the characteristic absorption bands for pure PVA, pure chitosan, and the additional absorption bands characteristic of PEO and of chlorhexidine. The additional band of PEO appears at 1,644 cm^{-1}, which is attributed to the C=O stretching vibration. Bending vibration shown at 1,375 cm^{-1} is related to the O–H bond. Deformation vibration shown at 1,465 and 1,342 cm^{-1} is related to C–H bonds. Bending vibration shown at 1,278 and 1,237 cm^{-1} is related to the O–H bonds. Stretching vibration shown at 1,140 cm^{-1} is related to the C–O bond.[42] The additional band characteristic of chlorhexidine appears at 1,492 cm^{-1}, which is related to the chlorophenol groups of chlorhexidine.[41]

TGA
TGA for the upper layer of the fabricated mat
Figure 6 shows the TGA results for the following samples: pure PVA, pure chitosan, PVA/chitosan, PVA/chitosan/
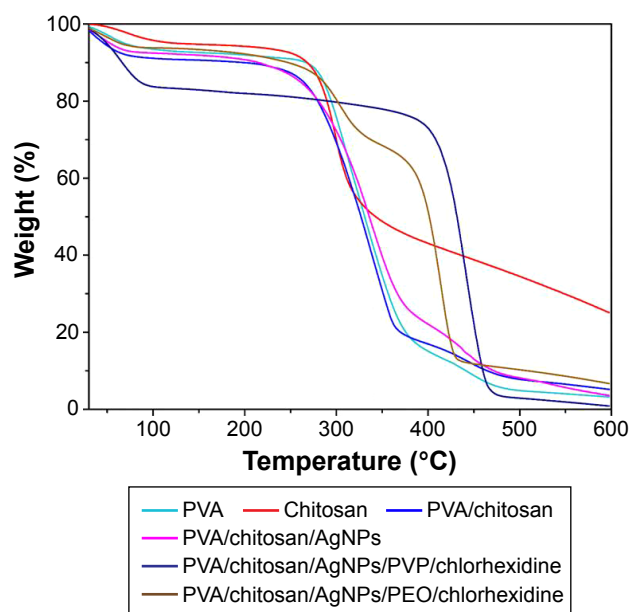

Figure 5 Comparative result of FT-IR spectra for all fabricated samples.
Notes: FT-IR shown is for (**A**) PVA, (**B**) chitosan, (**C**) PVA/chitosan, (**D**) PVA/ chitosan/AgNPs, (**E**) PVA/chitosan/AgNPs/PVP/chlorhexidine, and (**F**) PVA/chitosan/ AgNPs/PEO/chlorhexidine.
Abbreviations: FT-IR, Fourier transform infrared spectroscopy; PVA, poly(vinyl alcohol); AgNPs, silver nanoparticles; PVP, polyvinylpyrrolidone; PEO, polyethylene oxide.

Figure 6 Comparative result of TGA spectra for all samples.
Notes: TGA shown is for PVA, chitosan, PVA/chitosan, PVA/chitosan/AgNPs, PVA/ chitosan/AgNPs/PVP/chlorhexidine, and PVA/chitosan/AgNPs/PEO/chlorhexidine.
Abbreviations: TGA, thermogravimetric analysis; PVA, poly(vinyl alcohol); AgNPs, silver nanoparticles; PVP, polyvinylpyrrolidone; PEO, polyethylene oxide.

AgNPs, PVP–drug-loaded double layer, and PEO–drug-loaded double layer.

The decomposition of PVA undergoes three stages. First, the initial weight loss at 50°C–170°C is attributed to moisture vaporization. Second, a weight loss begins at 240°C, which is related to the decomposition of the side chain of PVA. In the third stage, starting at 400°C, further degradation takes place for polyene residues that result in carbon and hydrocarbons.[43] The decomposition of chitosan undergoes three stages. First, weight loss at 40°C–140°C is attributed to the moisture vaporization. The second stage of weight loss starts at 230°C. This corresponds to more strongly linked structural water. At the third stage, at 320°C, the weight loss is related to the degradation of polymeric chains of chitosan.[39] The sample shows slightly higher thermal stability that could correspond to the presence of the metal (AgNPs).

TGA for the PVP–drug-loaded double layer

Initially, PVA/chitosan/AgNPs/PVP/chlorhexidine showed a weight loss at 50°C–100°C, which is attributed to the moisture vaporization. Thermal degradation of the sample shows a behavior that resembles that of PVP found in literature.[44] PVP could be dominant as it has the highest thermal stability in comparison to other constituents in the sample. The major weight loss between 380°C and 460°C can be assigned to normal thermal decomposition of PVP. The last weight loss over 470°C can be attributed to the elimination of carbon residues and embedded organic fragments, resulting from the thermal reactions. This composition was found to have the highest thermal stability.

TGA for PEO–drug-loaded double layer

After the initial weight loss between 50°C and 100°C, due to moisture vaporization, decomposition of PVA/chitosan/AgNPs/PEO/chlorhexidine showed other weight losses at 230°C and between 340°C and 420°C. According to the literature,[45] decomposition of PEO happens between 340°C and 420°C. Weight loss at ~230°C could correspond to the PVA and chitosan decomposition. This system showed higher thermal stability in comparison with the PVA/chitosan/AgNP layer.

XRD

Peak indexing

Indexing (determination of the unit cell dimensions through peak positioning) is the principal step in the analysis of a diffraction pattern. The XRD pattern of PVA/chitosan/AgNPs is shown in Figure 7. There are four diffraction peaks observed at 38.57°, 44.6°, 65.1°, and 78.2° in the 2θ range 20°–80° of the sample. These peaks can be assigned
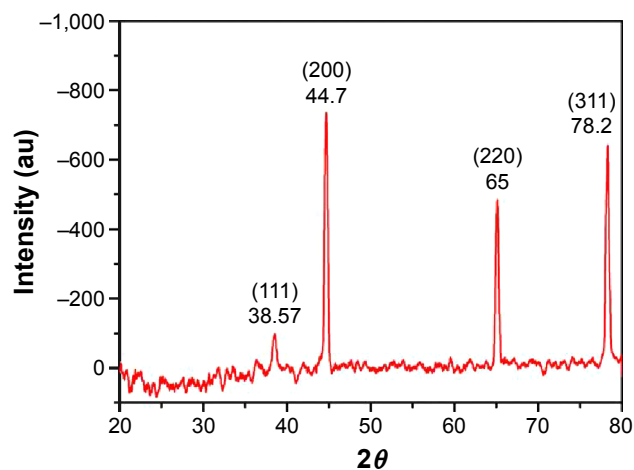

Figure 7 XRD spectra for electrospun PVA/chitosan/AgNPs.
Note: The four diffraction peaks are ascribed to corresponding reflection planes of FCC structure of Ag phase.
Abbreviations: XRD, X-ray diffraction; PVA, poly(vinyl alcohol); AgNPs, silver nanoparticles; FCC, face-centered cubic; au, atomic unit; Ag, silver.

to the (111), (200), (220), and (311) reflection planes of the face-centered cubic structure of Ag phases, respectively.[46,47] The results observed were matched with the standard powder diffraction card of Joint Committee on Powder Diffraction Standards, silver file no 04-0783, which prove that the particles obtained are AgNPs (Table 1).[48]

Particle size calculations

The average particle size was calculated (approximately) by using the Debye-Scherrer formula:[49]

$$D = \frac{0.9\lambda}{\beta cos\theta} \qquad (1)$$

where D is the particle diameter size, λ is the wavelength of the X-ray (0.1541 nm), β is the full width at half maximum, and θ is the diffraction angle. The particles sizes obtained ranged from 16.23 to 20.89 nm, the details of which are listed in Table 2.

Antimicrobial susceptibility test

For antimicrobial assessment, the prepared samples were tested against four microorganisms, *S. aureus* (Gram-positive

Table 1 Comparison of experimental and standard diffraction angles for AgNPs

Experimental diffraction angle (2θ in degrees)	Standard diffraction angle (2θ in degrees), JCPDS silver: 04-0783
38.57	38.116
44.7	44.277
65	64.426
78.2	77.472

Abbreviations: AgNPs, silver nanoparticles; JCPDS, Joint Committee on Powder Diffraction Standards.

Table 2 Calculated grain size for AgNPs

2θ of the intense peak (degrees)	Miller indices (hkl)	θ of the intense peak (degrees)	FWHM of intense peak (β), radians	Size of the particle (D), nm
38.57	(111)	19.29	0.0094	16.23
44.7	(200)	22.35	0.0077	19.33
65	(220)	32.50	0.0073	20.89
78.2	(311)	39.10	0.0084	18.26

Abbreviations: AgNPs, silver nanoparticles; FWHM, full width at half maximum.

cocci), *E. coli* and *P. aeruginosa* (Gram-negative rods), and *C. albicans* (pathogenic skin yeast), using the agar diffusion method as described previously to assess their antimicrobial activity. The inhibition zone produced by each sample was measured. Figure 8 shows PVA/chitosan (control), PVA/chitosan/AgNPs, PVP–drug-loaded, and PEO–drug-loaded samples against *S. aureus*, *E. coli*, *P. aeruginosa*, and *C. albicans*. It was found that PVA/chitosan sample did not exhibit any antibacterial activity against any of the tested microorganisms. PVA/chitosan/AgNPs showed inhibition against all tested microorganisms. The strongest activity was against *S. aureus* (18 mm), followed by *E. coli* and *C. albicans* (15 mm) and then by *P. aeruginosa* (10 mm). The antimicrobial activity of AgNPs is known to work via different mechanisms,[50] such as releasing reactive oxygen species that destruct the cellular membrane, physical contact

Figure 8 Antimicrobial susceptibility disk diffusion test.
Notes: (1) PVA/chitosan (control), (2) PVA/chitosan/AgNPs, (3) PVP-drug loaded, and (4) PEO–drug loaded against (**A**) *Staphylococcus aureus*, (**B**) *Escherichia coli*, (**C**) *Pseudomonas aeruginosa*, and (**D**) *Candid albicans*.
Abbreviations: PVA, poly(vinyl alcohol); AgNPs, silver nanoparticles; PVP, polyvinylpyrrolidone; PEO, polyethylene oxide.

of the AgNP into the microbe provoking cellular damage,[51] and silver ion release into the microorganisms that interfere with its cellular activity and DNA replication.[34]

Chlorhexidine loaded on PVP showed antimicrobial inhibition against all tested microorganisms. The strongest activity was against *S. aureus* (16 mm) followed by *E. coli* (14 mm), *C. albicans* (12 mm), and then *P. aeruginosa* (10 mm). Chlorhexidine works against a broad spectrum of bacteria and fungi by reacting with the negatively charged phosphate groups found on the cell membrane of the microorganisms. This interference causes leakage of cytoplasmic chemicals, membrane destruction, and inhibition of enzyme activity inside the microbe.[52] Chlorhexidine loaded on PEO showed antibacterial inhibition against all tested microorganisms. The strongest activity was against *S. aureus* (21 mm), followed by *E. coli*, *C. albicans* (17 mm), and then *P. aeruginosa* (10 mm).

It can be observed that the drug loaded on PEO showed higher antibacterial activity in comparison to the drug loaded on PVP. This may be related to the interaction of PEO or PVP with the drug. From the chemical structures of the compounds, it is expected that PVP and the drug will have a hydrogen-bonded interaction between –C=O on PVP and H–N– on the drug. Hence, PVP interaction with the drug is stronger than PEO interaction with the drug. This allows easier drug release from the PEO–drug-loaded nanofibers mat, causing an enhanced antibacterial activity in comparison to PVP–drug-loaded nanofiber mats.

Of importance, all antibacterial active samples in this study, PVA/chitosan/AgNPs, PVP/chlorhexidine, and PEO/chlorhexidine, were shown to have the strongest activity against *S. aureus*. On the other hand, the microorganism that thrived the most in the presence of these samples was *P. aeruginosa* (Figure 9).

Conclusion

In this study, two novel wound dressing nanofibers with a dual function were prepared. The design for both dressings consisted of the same system: two electrospun layers loaded with the same drug. The external upper layer, PVA/chitosan/AgNPs, was a common layer in both systems, which faced the environment. The lower layer, containing chlorhexidine, an antibiotic drug, was uploaded into a polymer. In one system, the antibiotic drug was uploaded on PVP, while in the other system, the drug was uploaded on PEO. The designed polymer system was fabricated via the electrospinning technique, which was chosen because of the beneficial properties obtained when creating a wound dressing that consisted of nanofibers.
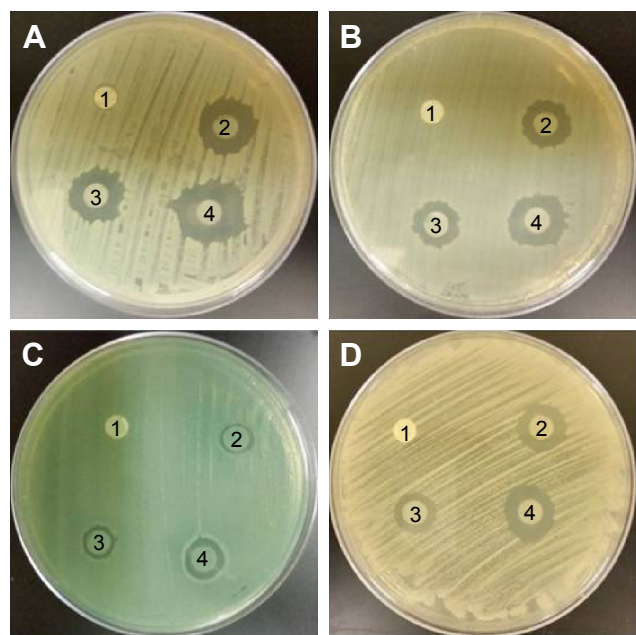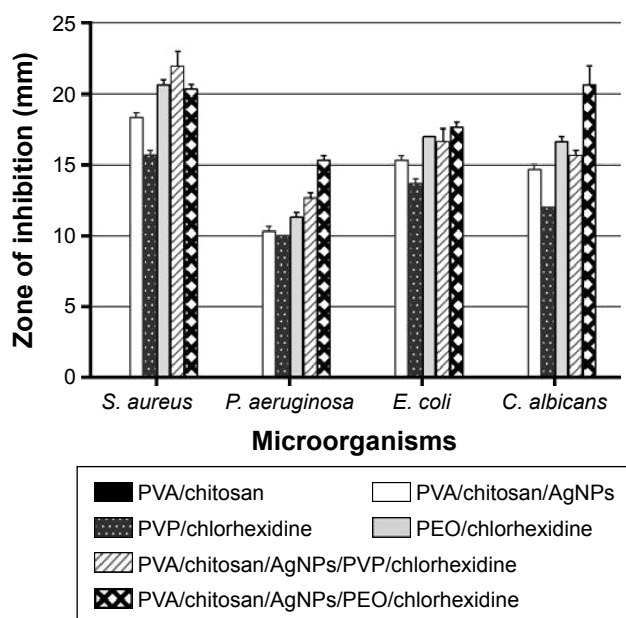
Figure 9 Diameter of zones of inhibition for PVA/chitosan, PVA/chitosan/AgNPs, PVP/chlorhexidine, and PEO/chlorhexidine against *S. aureus*, *P. aeruginosa*, *E. coli*, and *C. albicans*.
Abbreviations: PVA, poly(vinyl alcohol); AgNPs, silver nanoparticles; PVP, polyvinylpyrrolidone; PEO, polyethylene oxide; *S. aureus*, *Staphylococcus aureus*; *P. aeruginosa*, *Pseudomonas aeruginosa*; *E. coli*, *Escherichia coli*; *C. albicans*, *Candida albicans*.

The upper layer of the wound dressing was designed to act as a barrier against microbial invasion that could infect the wound. Its ability to act against microorganisms comes from the antibacterial activity of AgNPs. The lower layer acts as a drug release to the wound site. This ensures that the wounds get treated with minimum exposure to the environment, in comparison to the process of applying a typical drug followed by the process of dressing the wound.

The approach in fabricating the nanofibers was morphology oriented, and the samples were characterized, their antibacterial activities were investigated, and the chain motion dynamics and interfacial interactions of the selected materials were studied. FT-IR measurements showed incorporation of the blends. TGA showed the highest stability in the complete double layer system, while the system containing PVP had the highest stability of all. XRD characterization confirmed the reduction of silver nitrate to AgNPs through its interaction with chitosan.

The antibacterial assessment indicated that both systems have antibacterial activity against different types of microorganisms: *E. coli* and *P. aeruginosa* (Gram-negative rods), *S. aureus* (Gram-positive cocci), and *C. albicans* (yeast). Although both showed activity, the drug system containing PEO proved to have higher antibacterial activity than the drug system containing PVP. PVA/chitosan/AgNPs did show antibacterial activity as well, which supports their intended role as a barrier against environmental contamination.

References
1. Abrigo M, McArthur SL, Kingshott P. Electrospun nanofibers as dressings for chronic wound care: advances, challenges, and future prospects. *Macromol Biosci*. 2014;14(6):772–792.
2. Li M, Mondrinos MJ, Gandhi MR, Ko FK, Weiss AS, Lelkes PI. Electrospun protein fibers as matrices for tissue engineering. *Biomaterials*. 2005;26(30):5999–6008.
3. Pham QP, Sharma U, Mikos AG. Electrospun poly (epsilon-caprolactone) microfiber and multilayer nanofiber/microfiber scaffolds: characterization of scaffolds and measurement of cellular infiltration. *Biomacromolecules*. 2006;7(10):2796–2805.
4. Shao S, Li L, Yang G, et al. Controlled green tea polyphenols release from electrospun PCL/MWCNTs composite nanofibers. *Int J Pharm*. 2011;421(2):310–320.
5. Ignatova M, Rashkov I, Manolova N. Drug-loaded electrospun materials in wound-dressing applications and in local cancer treatment. *Expert Opin Drug Deliv*. 2013;10(4):469–483.
6. Moreno I, González-González V, Romero-García J. Control release of lactate dehydrogenase encapsulated in poly (vinyl alcohol) nanofibers via electrospinning. *Eur Polym J*. 2011;47(6):1264–1272.
7. Charernsriwilaiwat N, Rojanarata T, Ngawhirunpat T, Opanasopit P. Electrospun chitosan/polyvinyl alcohol nanofibre mats for wound healing. *Int Wound J*. 2014;11(2):215–222.
8. Varshosaz J, Jannesari M, Morshed M, Zamani M. Composite poly(vinyl alcohol)/poly(vinyl acetate) electrospun nanofibrous mats as a novel wound dressing matrix for controlled release of drugs. *Int J Nanomedicine*. 2011;6:993.
9. Abdelgawad AM, Hudson SM, Rojas OJ. Antimicrobial wound dressing nanofiber mats from multicomponent (chitosan/silver-NPs/polyvinyl alcohol) systems. *Carbohydr Polym*. 2014;100:166–178.
10. Hassiba AJ, El Zowalaty ME, Nasrallah GK, et al. Review of recent research on biomedical applications of electrospun polymer nanofibers for improved wound healing. *Nanomedicine (Lond)*. 2016;11(6):715–737.
11. Gholipour Kanani A, Hajir Bahrami S. Review on electrospun nanofibres scaffold and biomedical applications. *Trends Biomater Artif Organs*. 2010;24(2):93–115.
12. Bhattarai N, Edmondson D, Veiseh O, Matsen FA, Zhang M. Electrospun chitosan-based nanofibers and their cellular compatibility. *Biomaterials*. 2005;26(31):6176–6184.
13. Shan YH, Peng LH, Liu X, Chen X, Xiong J, Gao JQ. Silk fibroin/gelatin electrospun nanofibrous dressing functionalized with astragaloside IV induces healing and anti-scar effects on burn wound. *Int J Pharm*. 2015;479(2):291–301.
14. Stone SA, Gosavi P, Athauda TJ, Ozer RR. In situ citric acid crosslinking of alginate/polyvinyl alcohol electrospun nanofibers. *Mater Lett*. 2013;112:32–35.
15. Wang M, Fang D, Wang N, et al. Preparation of PVDF/PVP core-shell nanofibers mats via homogeneous electrospinning. *Polymer*. 2014;55(9):2188–2196.
16. Tan L, Hu J, Zhao H. Design of bilayered nanofibrous mats for wound dressing using an electrospinning technique. *Mater Lett*. 2015;156:46–49.
17. Sirc J, Kubinova S, Hobzova R, et al. Controlled gentamicin release from multi-layered electrospun nanofibrous structures of various thicknesses. *Int J Nanomedicine*. 2012;7:5315–5325.

18. Chen DWC, Liao JY, Liu SJ, Chan EC. Novel biodegradable sandwich-structured nanofibrous drug-eluting membranes for repair of infected wounds: an in vitro and in vivo study. *Int J Nanomedicine*. 2012;7: 763–771.

19. Yang JM, Yang SJ, Lin HT, Wu T-H, Chen H-J. Chitosan containing PU/Poly(NIPAAm) thermosensitive membrane for wound dressing. *Mater Sci Eng C*. 2008;28(1):150–156.

20. Xie Y, Liu X, Chen Q. Synthesis and characterization of water-soluble chitosan derivate and its antibacterial activity. *Carbohydr Polym*. 2007; 69(1):142–147.

21. Dragostin OM, Samal SK, Dash M, et al. New antimicrobial chitosan derivatives for wound dressing applications. *Carbohydr Polym*. 2016; 141:28–40.

22. Hadipour-Goudarzi E, Montazer M, Latifi M, Aghaji AA. Electrospinning of chitosan/sericin/PVA nanofibers incorporated with in situ synthesis of nano silver. *Carbohydr Polym*. 2014;113:231–239.

23. Hang AT, Tae B, Park JS. Non-woven mats of poly(vinyl alcohol)/chitosan blends containing silver nanoparticles: fabrication and characterization. *Carbohydr Polym*. 2010;82(2):472–479.

24. Naseri N, Algan C, Jacobs V, John M, Oksman K, Mathew AP. Electrospun chitosan-based nanocomposite mats reinforced with chitin nanocrystals for wound dressing. *Carbohydr Polym*. 2014;109:7–15.

25. Kamoun EA, Chen X, Mohy Eldin MS, Kenawy ERS. Crosslinked poly(vinyl alcohol) hydrogels for wound dressing applications: a review of remarkably blended polymers. *Arab J Chem*. 2014;8(1):1–14.

26. Li CW, Fu RQ, Yu CP, et al. Silver nanoparticle/chitosan oligosaccharide/poly(vinyl alcohol) nanofibers as wound dressings: a preclinical study. *Int J Nanomedicine*. 2013;8:4131–4145.

27. Ruszczak Z. Effect of collagen matrices on dermal wound healing. *Adv Drug Deliv Rev*. 2003;55(12):1595–1611.

28. Aoyagi S, Onishi H, Machida Y. Novel chitosan wound dressing loaded with minocycline for the treatment of severe burn wounds. *Int J Pharm*. 2007;330(1–2):138–145.

29. Denkbaş EB, Oztürk E, Ozdemir N, Keçeci K, Agalar C. Norfloxacin-loaded chitosan sponges as wound dressing material. *J Biomater Appl*. 2004;18(4):291–303.

30. Chen L, Bromberg L, Hatton TA, Rutledge GC. Electrospun cellulose acetate fibers containing chlorhexidine as a bactericide. *Polymer (Guildf)*. 2008;49(5):1266–1275.

31. Scaffaro R, Botta L, Sanfilippo M, Gallo G, Palazzolo G, Puglia AM. Combining in the melt physical and biological properties of poly(caprolactone) and chlorhexidine to obtain antimicrobial surgical monofilaments. *Appl Microbiol Biotechnol*. 2013;97(1):99–109.

32. McDonnell G, Russell AD. Antiseptics and disinfectants: activity, action, and resistance. *Clin Microbiol Rev*. 1999;12(1):147–179.

33. Fernandes JG, Correia DM, Botelho G, et al. PHB-PEO electrospun fiber membranes containing chlorhexidine for drug delivery applications. *Polym Test*. 2014;34:64–71.

34. Wilkinson LJ, White RJ, Chipman JK. Silver and nanoparticles of silver in wound dressings: a review of efficacy and safety. *J Wound Care*. 2011; 20(11):543–549.

35. Ahamed M, Karns M, Goodson M, et al. DNA damage response to different surface chemistry of silver nanoparticles in mammalian cells. *Toxicol Appl Pharmacol*. 2008;233(3):404–410.

36. Usman MS, El Zowalaty ME, Shameli K, Zainuddin N, Salama M, Ibrahim NA. Synthesis, characterization, and antimicrobial properties of copper nanoparticles. *Int J Nanomedicine*. 2013;2013(8):4467–4479.

37. Schmitt J, Flemming H-C. FTIR-spectroscopy in microbial and material analysis. *Int Biodeterior Biodegradation*. 1998;41(1):1–11.

38. Mansur HS, Sadahira CM, Souza AN, Mansur AAP. FTIR spectroscopy characterization of poly (vinyl alcohol) hydrogel with different hydrolysis degree and chemically crosslinked with glutaraldehyde. *Mater Sci Eng C*. 2008;28(4):539–548.

39. Fernandes LL, Resende CX, Tavares DS, Soares GA, Castro LO, Granjeiro JM. Cytocompatibility of chitosan and collagen-chitosan scaffolds for tissue engineering. *Polímeros*. 2011;21(1):1–6.

40. Basha MA-F. Magnetic and optical studies on polyvinylpyrrolidone thin films doped with rare earth metal salts. *Polym J*. 2010;42(9):728–734.

41. Rema T, Lawrence JR, Dynes JJ, Hitchcock AP, Korber DR. Microscopic and spectroscopic analyses of chlorhexidine tolerance in Delftia acidovorans biofilms. *Antimicrob Agents Chemother*. 2014;58(10): 5673–5686.

42. Wang C, Feng L, Yang H, et al. Graphene oxide stabilized polyethylene glycol for heat storage. *Phys Chem Chem Phys*. 2012;14(38):13233.

43. Dassios KG. Poly (vinyl alcohol)-infiltrated carbon nanotube carpets. *Mater Sci Appl*. 2012;3(9):658–663.

44. Chai JH, Wu QS. Electrospinning preparation and electrical and biological properties of ferrocene/poly(vinylpyrrolidone) composite nanofibers. *Beilstein J Nanotechnol*. 2013;4:189–197.

45. Silva MF, da Silva CA, Fogo FC, Pineda EAG, Hechenleitner AAW. Thermal and FTIR study of polyvinylpyrrolidone/lignin blends. *J Therm Anal Calorim*. 2005;79:367–370.

46. Umadevi M, Shalini S, Bindhu MR. Synthesis of silver nanoparticle using *D. carota* extract. *Adv Nat Sci Nanosci Nanotechnol*. 2012;3(2): 1–6.

47. Bykkam S, Ahmadipour M, Narisngam S. Extensive studies on X-ray diffraction of green synthesized silver nanoparticles. *Adv Nanopart*. 2015;4:1–10.

48. Lanje AS, Sharma SJ, Pode RB. Synthesis of silver nanoparticles: a safer alternative to conventional antimicrobial and antibacterial agents. *J Chem Pharm Res*. 2010;2(3):478–483.

49. Hall BD, Zanchet D, Ugarte D. Estimating nanoparticle size from diffraction measurements. *J Appl Crystallogr*. 2000;33(6):1335–1341.

50. Eckhardt S, Brunetto PS, Gagnon J, Priebe M, Giese B, Fromm KM. Nanobio silver: its interactions with peptides and bacteria, and its uses in medicine. *Chem Rev*. 2013;113:4708–4754.

51. Kim JS, Kuk E, Yu KN, et al. Antimicrobial effects of silver nanoparticles. *Nanomedicine*. 2007;3:95–101.

52. Hope CK, Wilson M. Analysis of the effects of chlorhexidine on oral biofilm vitality and structure based on viability profiling and an indicator of membrane integrity. *Antimicrob Agents Chemother*. 2004; 48(5):1461–1468.